

**Electronic Supplementary Information for**

**Synthesis of high-entropy germanides and investigation of their formation process**

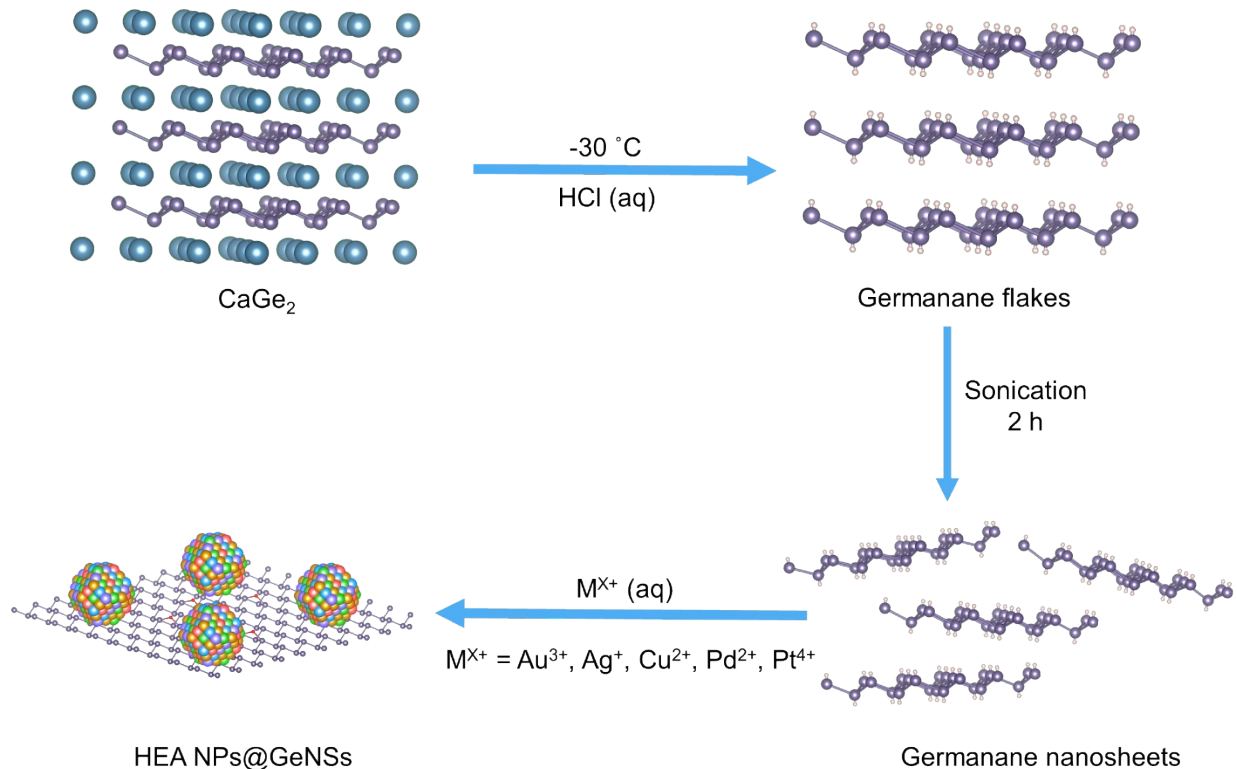
Chuyi Ni,<sup>a</sup> Kevin M. O'Connor,<sup>a</sup> Cole Butler<sup>a</sup> and Jonathan G. C. Veinot \*<sup>a</sup>

<sup>a</sup>Department of Chemistry, University of Alberta, Edmonton, Alberta T6G 2G2, Canada

**Table of Contents**

<b>Scheme S1.</b> A pictorial illustration of the formation of high-entropy nanoparticles on germanane. (Note: For clarity Ge-H moieties have been omitted in the HEA NPs@GeNSs illustration.) .....	3
<b>Figure S1.</b> A comparison of XRD patterns of HEA NPs@GeNSs and AuAgCuPdPtGe HEG. (*) correspond to GeO <sub>2</sub> reflections. Ge and GeO <sub>2</sub> reflections are from PDF#89-9345 and 83-2477. The asterisk corresponds to reflections arising from the impurities that from the synthesis of GeNSs. <sup>1</sup> .....	3
<b>Figure S2.</b> XRD peak broadening distribution for AuAgCuPdPtGe HEG.....	4
<b>Figure S3.</b> A plot of the lattice parameter as a function of the mole fraction of Ge in AuAgCuPdPtGe HEG by using Vegard's law. The red dot represents the experiment lattice parameter calculated from the XRD reflections using Bragg's law. .....	4
<b>Figure S4.</b> Representative FTIR spectra of HEA NPs@GeNSs before (black) and after (red) AuAgCuPdPtGe HEG formation. ....	5
<b>Figure S5.</b> Representative survey XP spectrum of AuAgCuPdPtGe HEG. ....	5
<b>Table S1.</b> Summary of XPS data for AuAgCuPdPtGe HEG.....	6
<b>Figure S6.</b> Representative high-resolution XP spectra of AuAgCuPdPtGe HEG: (a) Ge 3d, (b) Au 4f, (c) Ag 3d, (d) Cu 3d, (e) Pd 3d and Ge LMM, and (f) Pt 4f regions.....	6
<b>Figure S7.</b> Representative (a) average shifted histogram for AuAgCuPdPtGe HEG and (b) high-resolution TEM image of AuAgCuPdPtGe HEG showing GeO <sub>2</sub> (011) lattice spacing. (c) low-resolution bright-field TEM image of AuAgCuPdPtGe HEG. ....	7
<b>Figure S8.</b> A representative EDX spectrum for AuAgCuPdPtGe HEG. Mo signal results from the grid. ....	7
<b>Scheme S2.</b> A pictorial representation of the synthesis of FeCoNiCrVGe HEG. ....	8
<b>Figure S9.</b> A comparison of XRD patterns of metal salts&GeNSs precursor and FeCoNiCrVGe HEG. (*) correspond to GeO <sub>2</sub> reflections. Ge and GeO <sub>2</sub> reflections are from PDF#89-4562 and 83-2477.....	8
<b>Figure S10.</b> (a) XRD peak broadening distribution for the FeCoNiCrVGe HEG. (b) A plot of the lattice parameter as a function of the mole fraction of Ge in FeCoNiCrVGe HEG by using Vegard's law. The red dot represents the experiment lattice parameter calculated from the XRD reflections using Bragg's law. 9	9
<b>Figure S11.</b> Representative FTIR spectra of metal salts&GeNSs precursor (black) and FeCoNiCrVGe HEG (red). ....	9
<b>Figure S12.</b> Representative survey XP spectrum of FeCoNiCrVGe HEG. ....	10

<b>Figure S13.</b> Representative high-resolution XP spectra of FeCoNiCrVGe HEG: (a) Ge 3d, (b) V 2p, (c) Cr 2p, (d) Fe 2p, (e) Co 2p and (f) Ni 2p regions.....	10
<b>Table S2.</b> A summary of XPS data for liberated FeCoNiCrVGe HEG. ....	11
<b>Figure S14.</b> Representative (a) average shifted histogram for FeCoNiCrVGe HEG and (c) low-resolution bright-field TEM image of FeCoNiCrVGe HEG. ....	11
<b>Figure S15.</b> A representative EDX spectrum for FeCoNiCrVGe HEG.....	12
<b>Figure S16.</b> <i>In situ</i> heating XRD results of (a) AuAgCuPdPtGe HEG and (b) FeCoNiCrVGe HEG. (*) correspond to the reflections from the dome of <i>in situ</i> XRD heating stage. Ge and GeO <sub>2</sub> reflections are from PDF#89-3833 and 83-2477. ....	12
<b>Figure S17.</b> (a) Photograph of <i>in situ</i> XRD heating stage with the dome. (b) XRD pattern of the dome of <i>in situ</i> XRD heating stage. ....	13
<b>Figure S18.</b> (a) Average size of HEGs derived from the XRD results and (b) average size of HEA NPs and HEG derived from the TEM results. ....	13
<b>Figure S19.</b> A representative high-resolution XP spectrum of Ge 3d region of metal salts&GeNSs precursor. ....	14
<b>Figure S20.</b> Enhanced HAADF-STEM images of FeCoNiCrVGe HEG at the same location during the <i>in situ</i> heating experiment at 700 °C and 800 °C. (Boxes highlight regions where small metal nanoparticles arising from the reduction of excess metal salts have formed on the <i>in situ</i> heating nanochip.).....	14
<b>Figure S21.</b> Representative HAADF-STEM images and EDX mapping of metal salts&GeNSs. ....	15
<b>Figure S22.</b> A Representative EDX spectrum for metal salts&GeNSs. Si and N signals result from the Si <sub>3</sub> N <sub>4</sub> chip. ....	15
<b>Figure S23.</b> A representative HAADF-STEM images and EDX mapping of FeCoNiCrVGe HEG.....	16
<b>Figure S24.</b> A Representative EDX spectrum for FeCoNiCrVGe HEG. Si and N signals result from the Si <sub>3</sub> N <sub>4</sub> chip. ....	16
<b>Figure S25.</b> HAADF-STEM images of AuAgCuPdPtGe HEG at the same location during the <i>in situ</i> heating experiment from room temperature to 800 °C (a-g) and after cooling to room temperature (h). The sample shifted slightly due to thermal drift. ....	17
<b>Figure S26.</b> A representative HAADF-STEM images and EDX mapping of HEA NPs@GeNSs. ....	17
<b>Figure S27.</b> A representative EDX spectrum for HEA NPs@GeNSs. Si and N signals result from the Si <sub>3</sub> N <sub>4</sub> chip. ....	18
<b>Figure S28.</b> A representative HAADF-STEM images and EDX mapping of AuAgCuPdPtGe HEG.....	18
<b>Figure S29.</b> A representative EDX spectrum for AuAgCuPdPtGe HEG. Si and N signals result from the Si <sub>3</sub> N <sub>4</sub> chip. ....	19
<b>References.</b> .....	19



**Scheme S1.** A pictorial illustration of the formation of high-entropy nanoparticles on germanane.  
(Note: For clarity Ge-H moieties have been omitted in the HEA NPs@GeNSs illustration.)

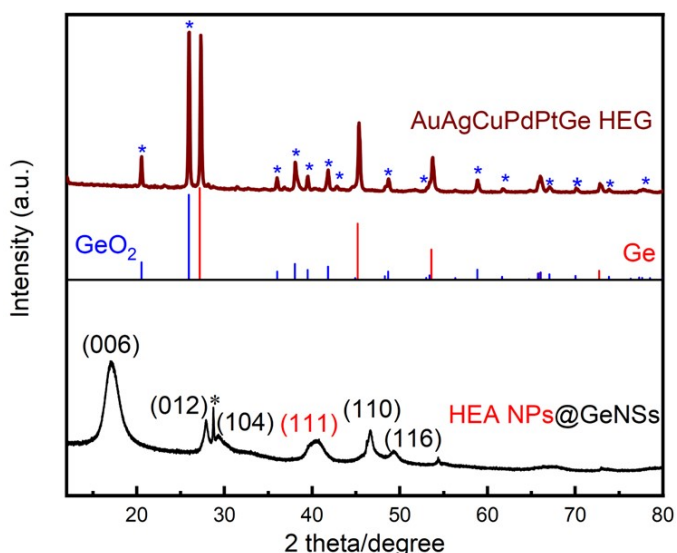


**Figure S1.** A comparison of XRD patterns of HEA NPs@GeNSs and AuAgCuPdPtGe HEG. (\*) correspond to  $\text{GeO}_2$  reflections. Ge and  $\text{GeO}_2$  reflections are from PDF#89-9345 and 83-2477. The asterisk corresponds to reflections arising from the impurities that from the synthesis of GeNSs.<sup>1</sup>

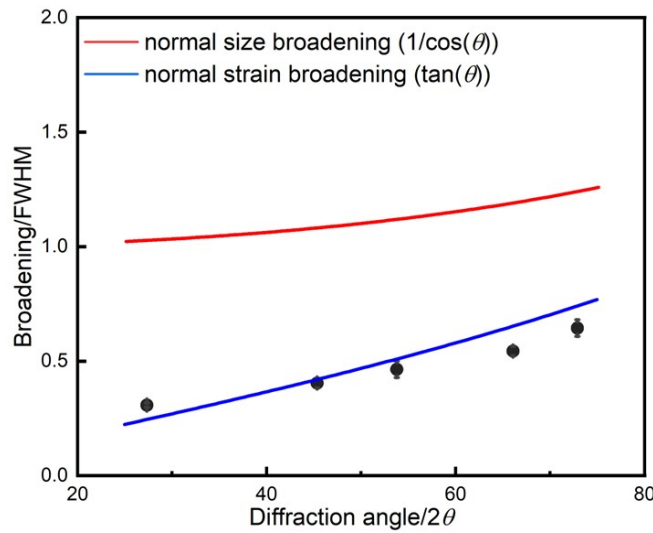


**Figure S2.** XRD peak broadening distribution for AuAgCuPdPtGe HEG.

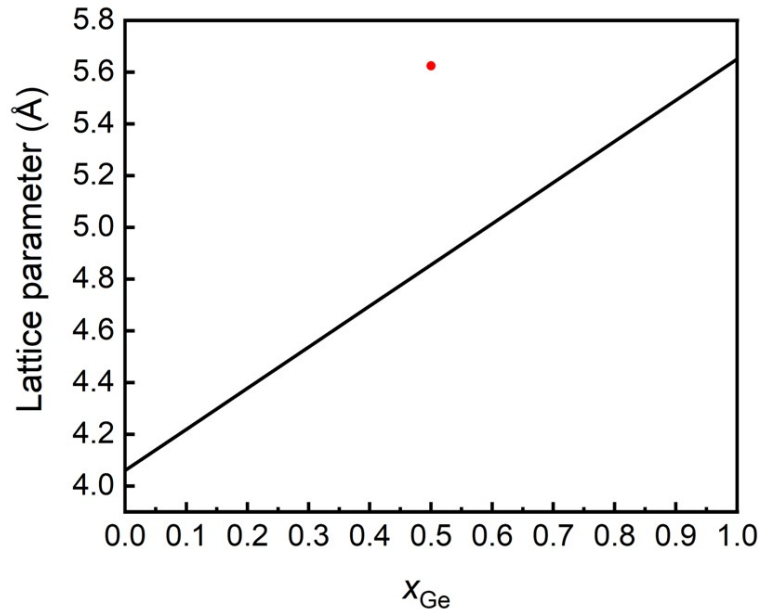


**Figure S3.** A plot of the lattice parameter as a function of the mole fraction of Ge in AuAgCuPdPtGe HEG by using Vegard's law. The red dot represents the experiment lattice parameter calculated from the XRD reflections using Bragg's law.

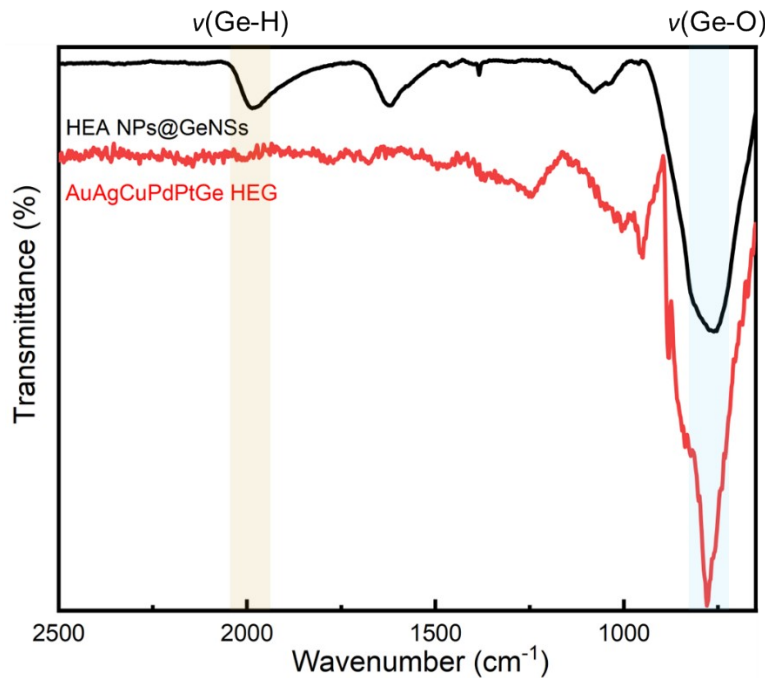


**Figure S4.** Representative FTIR spectra of HEA NPs@GeNSs before (black) and after (red) AuAgCuPdPtGe HEG formation.

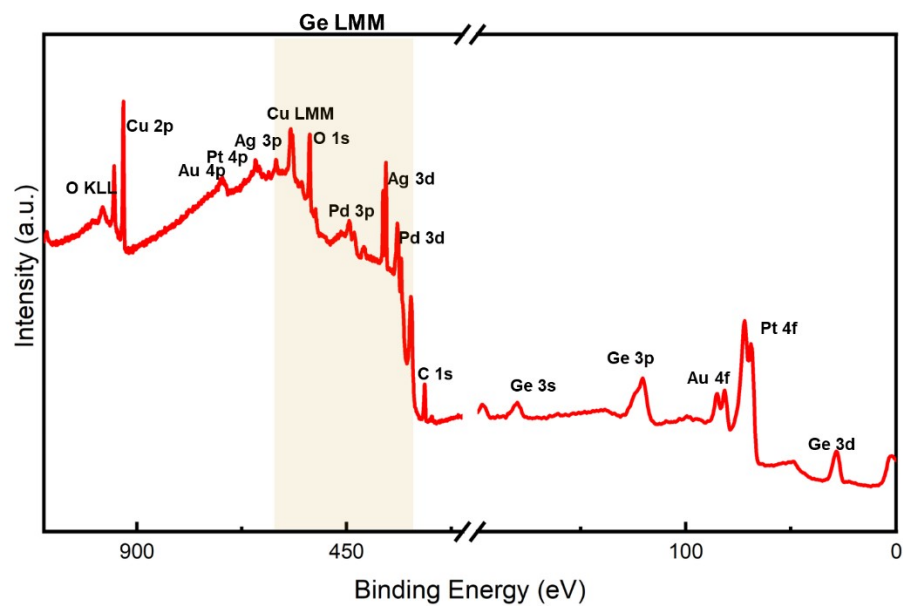


**Figure S5.** Representative survey XP spectrum of AuAgCuPdPtGe HEG.

**Table S1.** Summary of XPS data for AuAgCuPdPtGe HEG.

	Ge 3d	Au 4f	Ag 3d	Cu 2p	Pd 3d	Pt 4f
Emission (eV)	29.5	84.0	368.0	932.1	335.0	71.0
Reference emission (eV) <sup>a</sup>	29.8	84.0	368.2	933.0	335.0	71.0
Atomic percentage (%)	27.1	14.6	14.4	14.9	14.8	14.3
Electronegativity <sup>b</sup>	2.01	2.54	1.93	1.90	2.20	2.28

<sup>a</sup> Reference metal emissions are from NIST X-ray Photoelectron Spectroscopy Database.<sup>2</sup>

<sup>b</sup> Electronegativities are from CRC Handbook for Chemistry and Physics, 95th ed., 2014, CRC Press.<sup>3</sup>

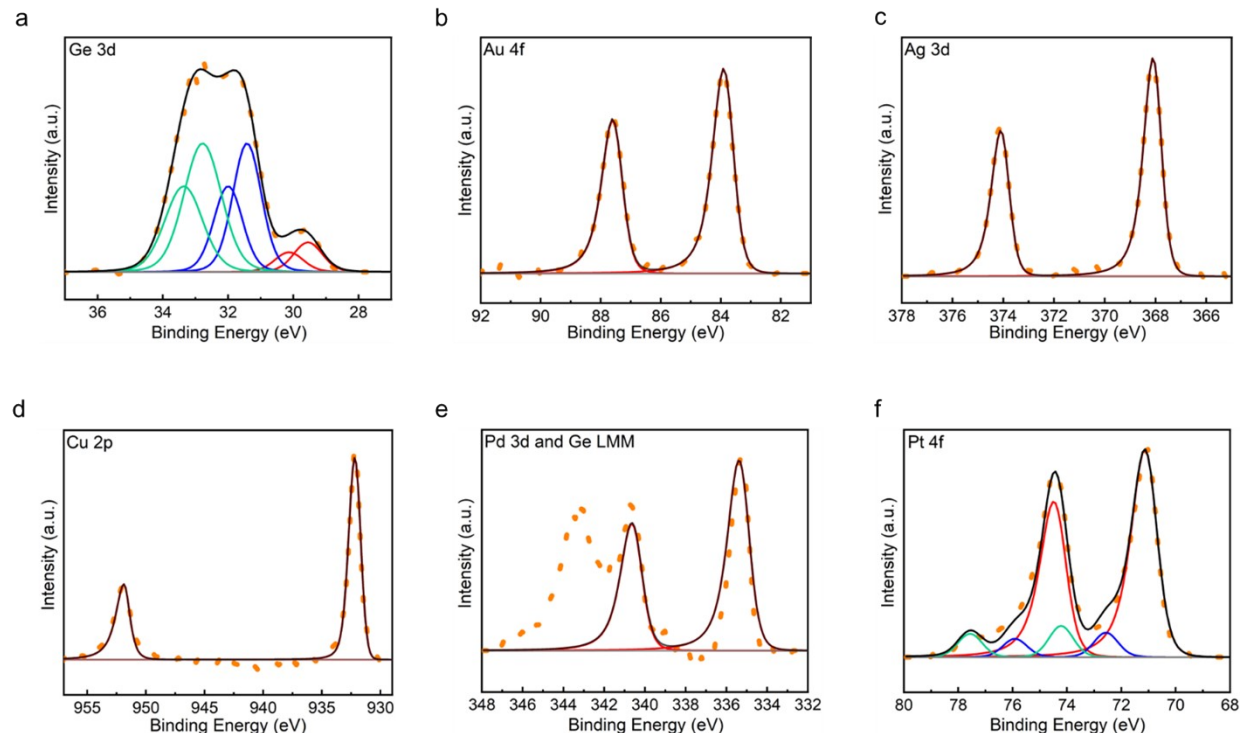


**Figure S6.** Representative high-resolution XP spectra of AuAgCuPdPtGe HEG: (a) Ge 3d, (b) Au 4f, (c) Ag 3d, (d) Cu 3d, (e) Pd 3d and Ge LMM, and (f) Pt 4f regions.

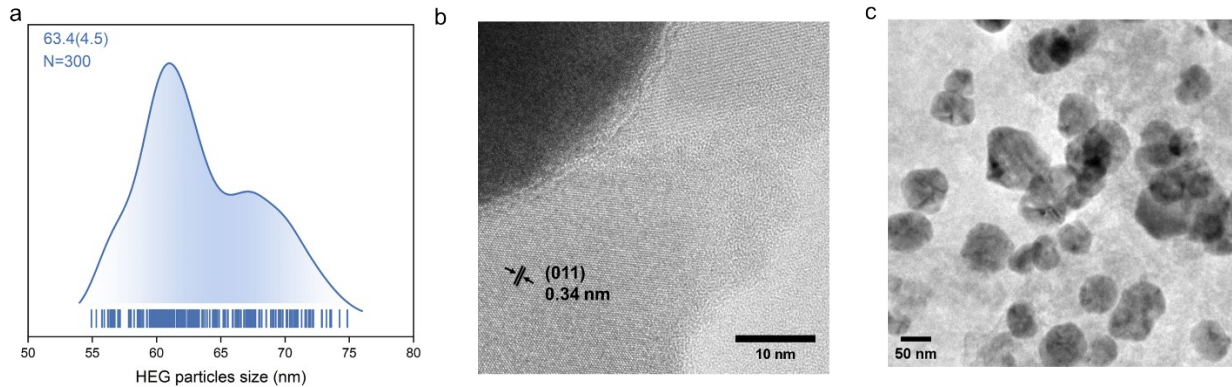


**Figure S7.** Representative (a) average shifted histogram for AuAgCuPdPtGe HEG and (b) high-resolution TEM image of AuAgCuPdPtGe HEG showing  $\text{GeO}_2$  (011) lattice spacing. (c) low-resolution bright-field TEM image of AuAgCuPdPtGe HEG.

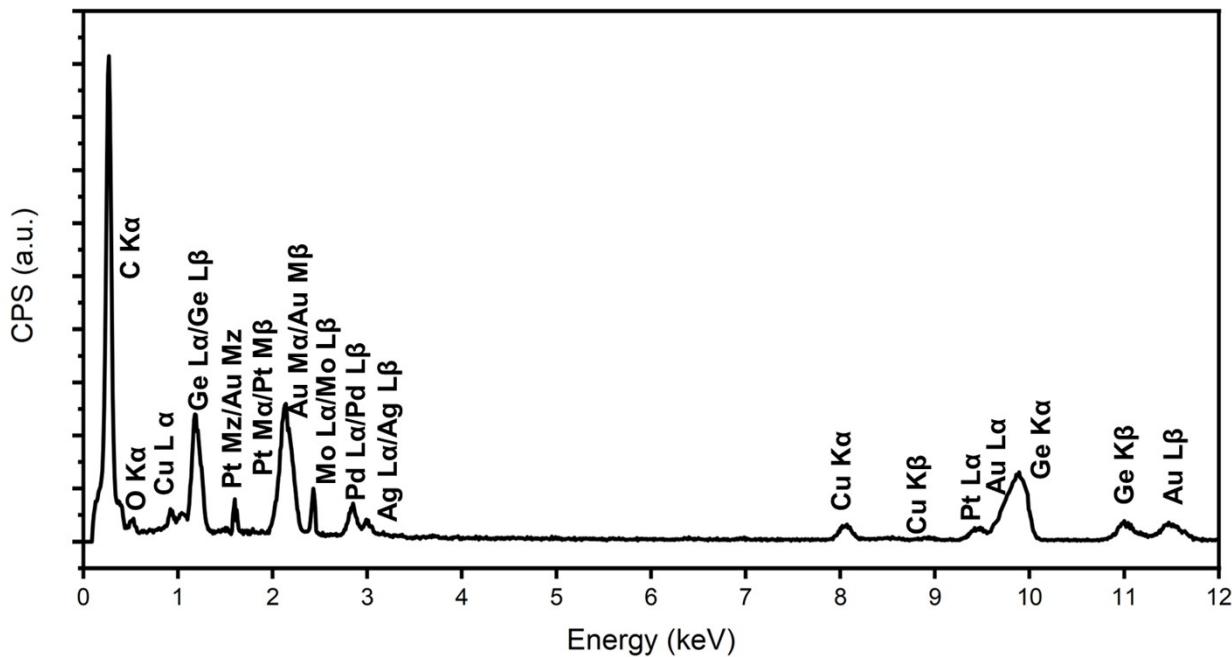
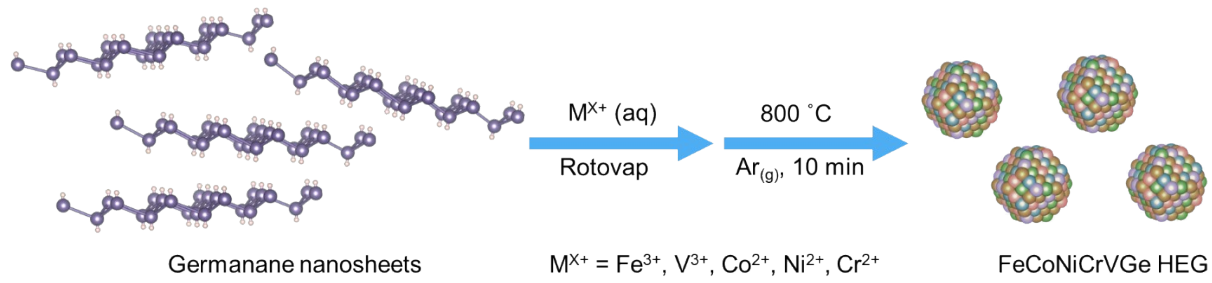


**Figure S8.** A representative EDX spectrum for AuAgCuPdPtGe HEG. Mo signal results from the grid.



**Scheme S2.** A pictorial representation of the synthesis of FeCoNiCrVGe HEG.

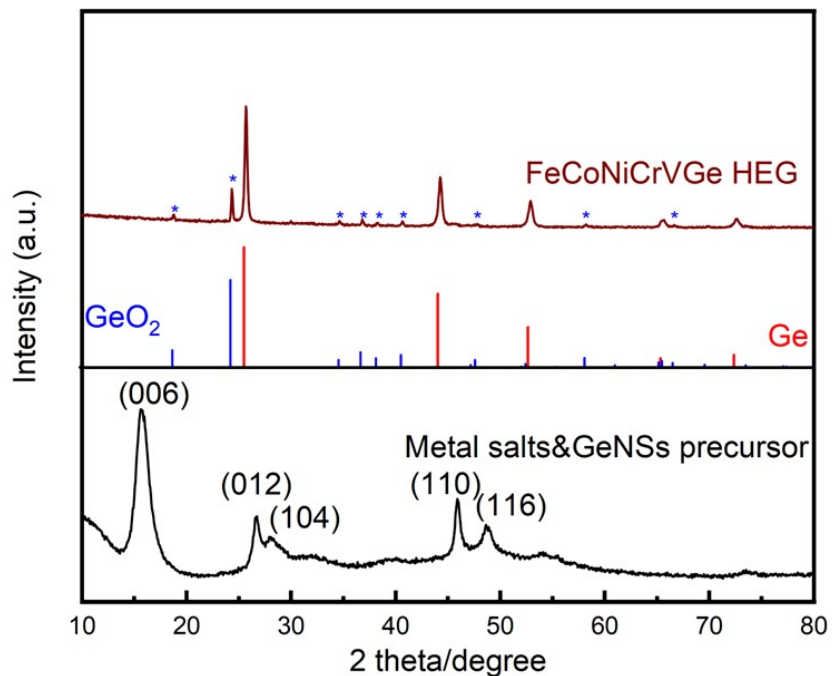


**Figure S9.** A comparison of XRD patterns of metal salts&GeNSs precursor and FeCoNiCrVGe HEG. (\*) correspond to GeO<sub>2</sub> reflections. Ge and GeO<sub>2</sub> reflections are from PDF#89-4562 and 83-2477.

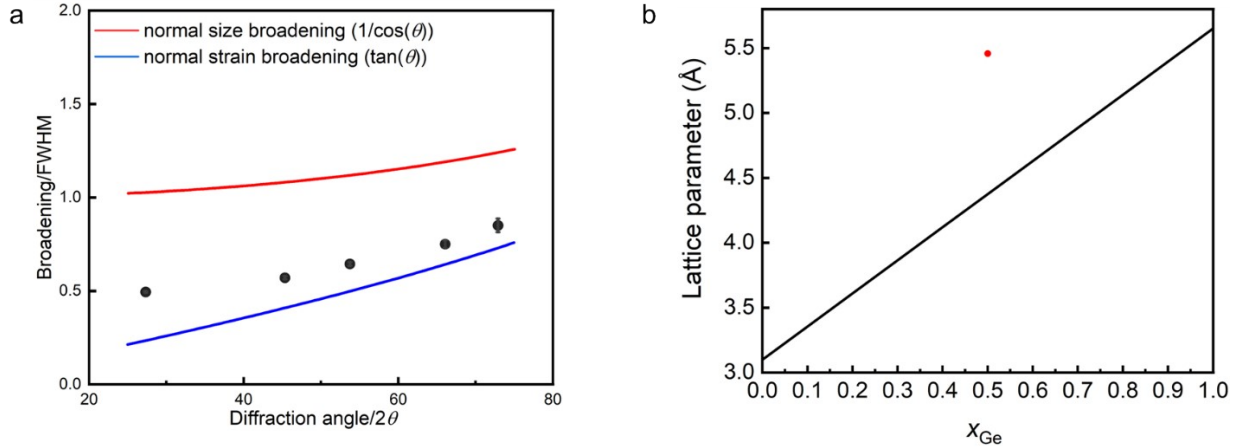


**Figure S10.** (a) XRD peak broadening distribution for the FeCoNiCrVGe HEG. (b) A plot of the lattice parameter as a function of the mole fraction of Ge in FeCoNiCrVGe HEG by using Vegard's law. The red dot represents the experiment lattice parameter calculated from the XRD reflections using Bragg's law.

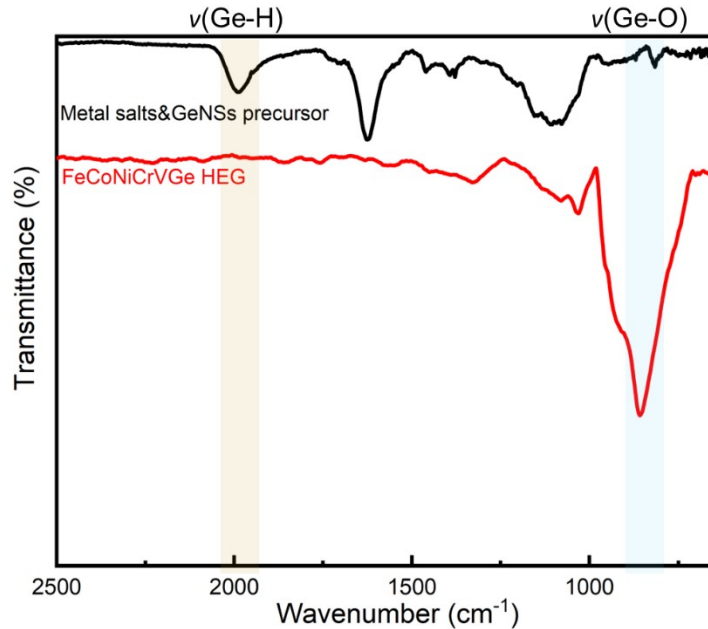


**Figure S11.** Representative FTIR spectra of metal salts&GeNSs precursor (black) and FeCoNiCrVGe HEG (red).

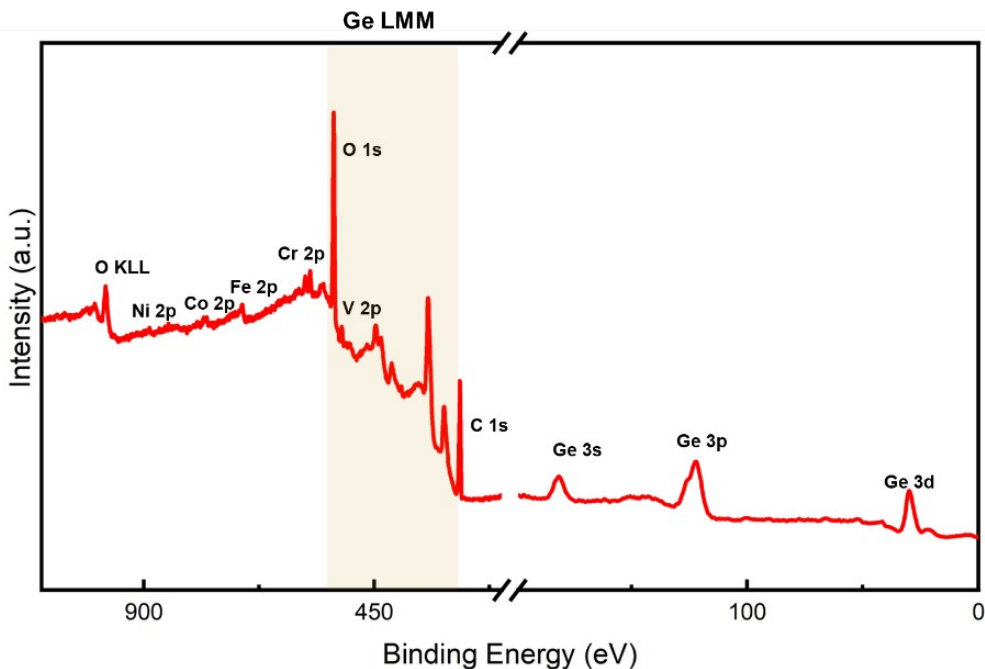


**Figure S12.** Representative survey XP spectrum of FeCoNiCrVGe HEG.

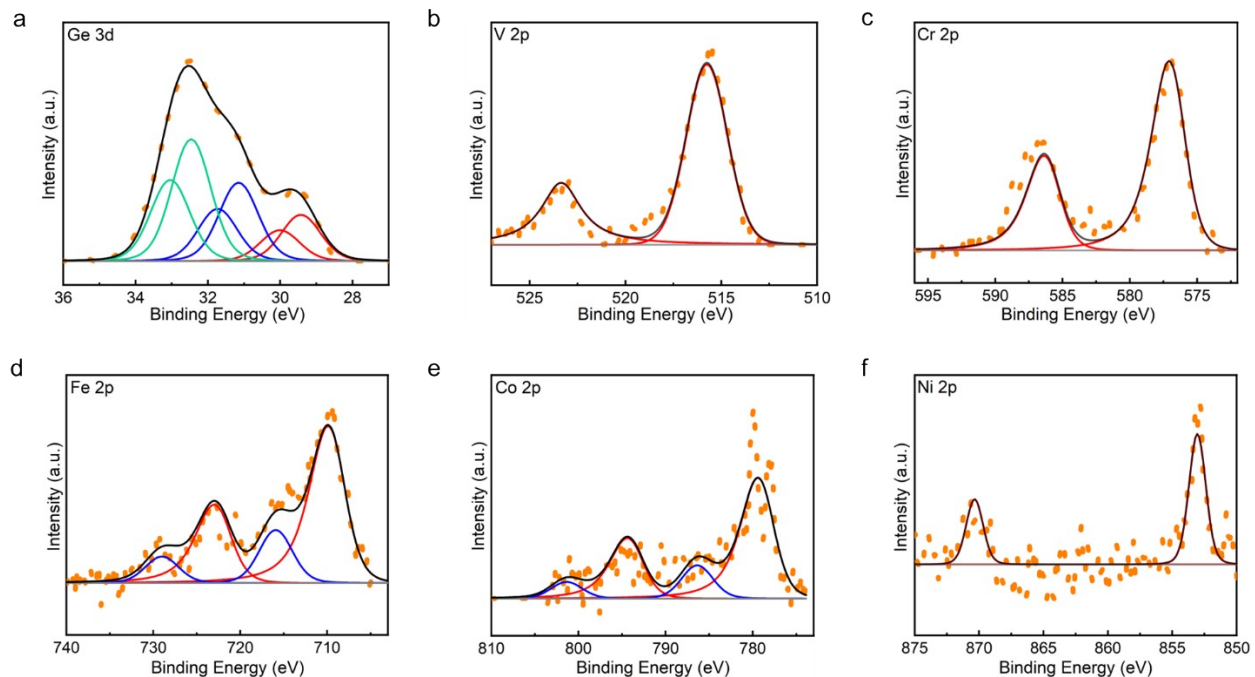


**Figure S13.** Representative high-resolution XP spectra of FeCoNiCrVGe HEG: (a) Ge 3d, (b) V 2p, (c) Cr 2p, (d) Fe 2p, (e) Co 2p and (f) Ni 2p regions.

**Table S2.** A summary of XPS data for liberated FeCoNiCrVGe HEG.

	Ge 3d	V 2p	Cr 2p	Fe 2p	Co 2p	Ni 2p
Emission (eV)	29.2	515.7	576.9	709.6	779.6	853.0
Reference emission (eV) <sup>a</sup>	29.5; Ge	515.7; V <sup>3+</sup>	576.9; Cr <sup>3+</sup>	709.6; Fe <sup>2+</sup>	779.6; Co <sup>2+</sup>	853.0; Ni <sup>+</sup>
Atomic percentage (%)	24.2	14.8	15.2	15.3	15.1	15.4
Eletronegativity <sup>b</sup>	2.01	1.63	1.66	1.83	1.88	1.91

<sup>a</sup> Reference metal emissions are from NIST X-ray Photoelectron Spectroscopy Database.<sup>2</sup>

<sup>b</sup> Eletronegativities are from CRC Handbook for Chemistry and Physics, 91st ed., 2010–2011, CRC Press.<sup>3</sup>

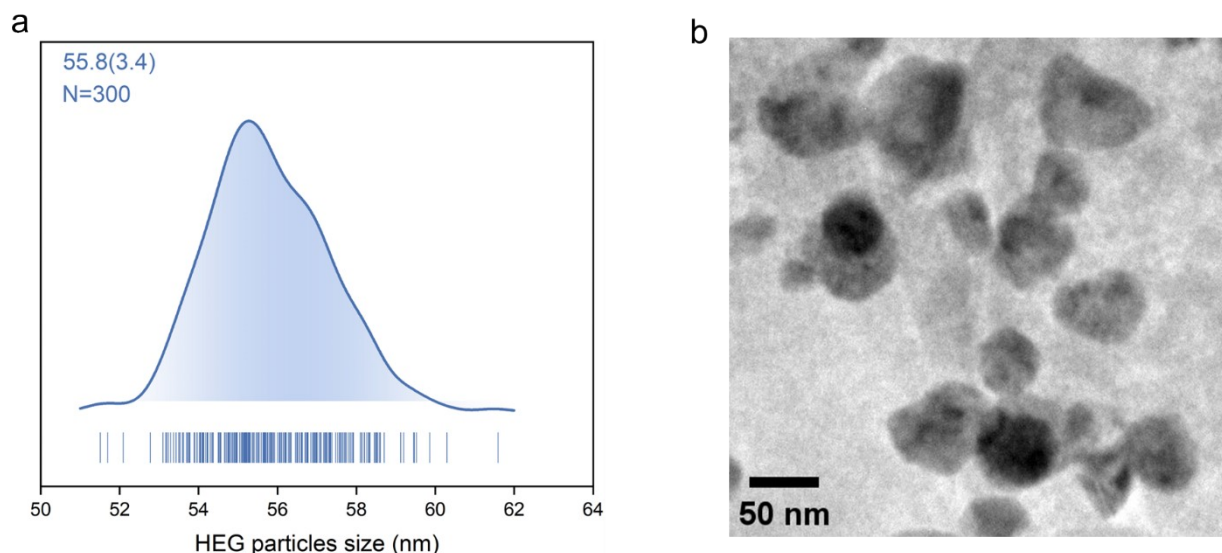


**Figure S14.** Representative (a) average shifted histogram for FeCoNiCrVGe HEG and (c) low-resolution bright-field TEM image of FeCoNiCrVGe HEG.

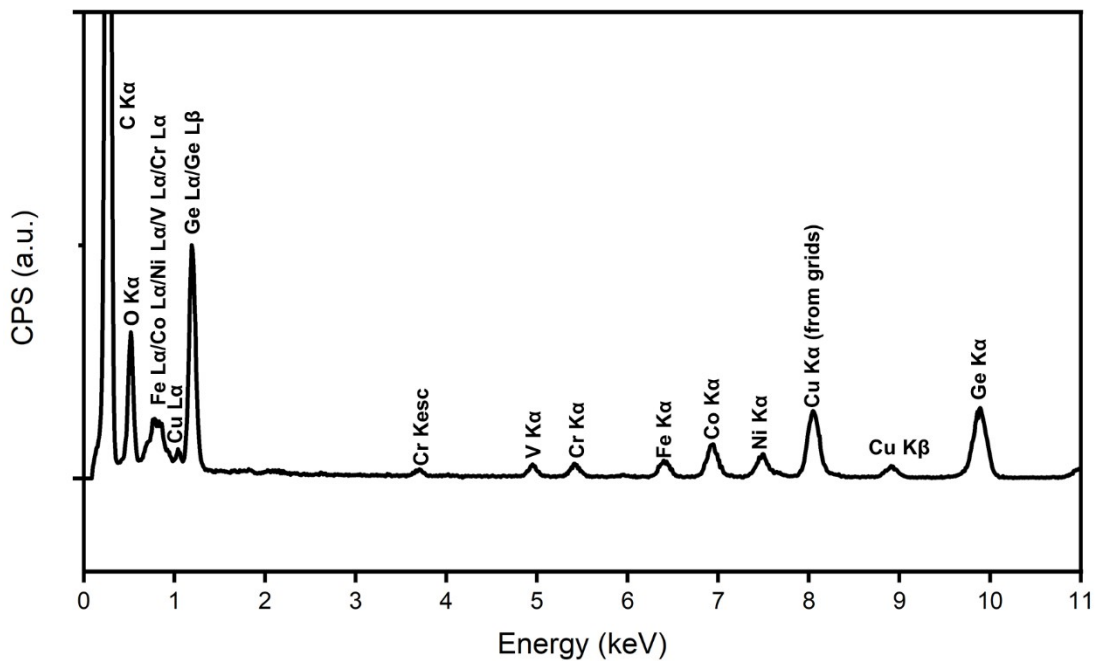


**Figure S15.** A representative EDX spectrum for FeCoNiCrVGe HEG.

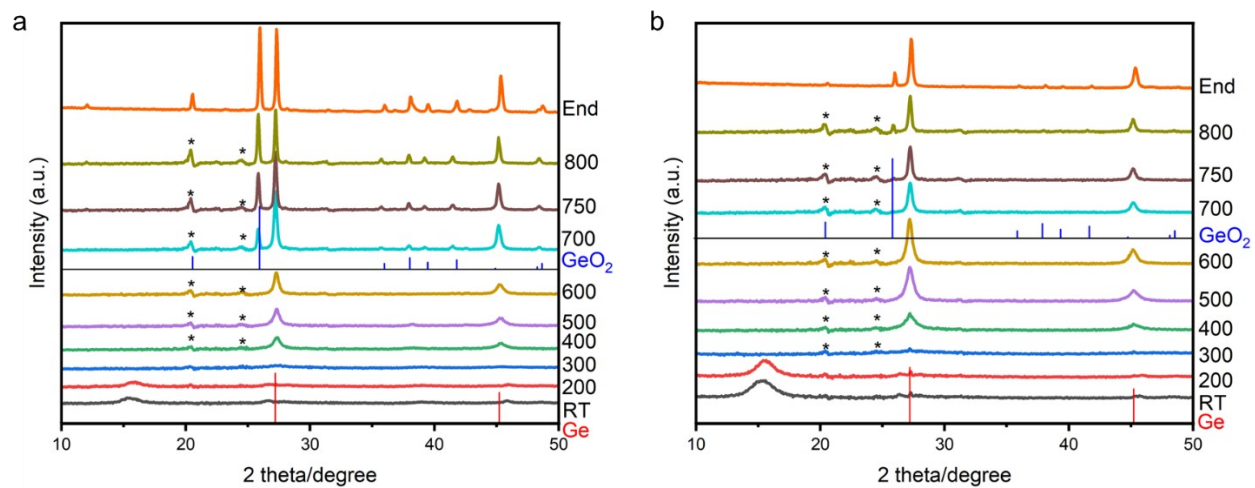


**Figure S16.** *In situ* heating XRD results of (a) AuAgCuPdPtGe HEG and (b) FeCoNiCrVGe HEG. (\*) correspond to the reflections from the dome of *in situ* XRD heating stage. Ge and  $\text{GeO}_2$  reflections are from PDF#89-3833 and 83-2477.

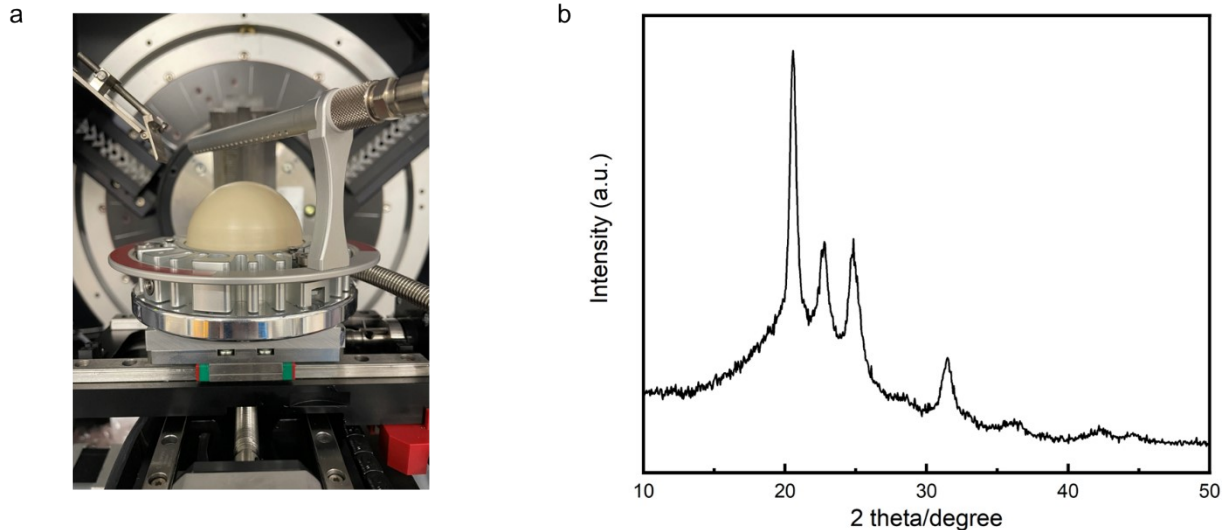


**Figure S17.** (a) Photograph of *in situ* XRD heating stage with the dome. (b) XRD pattern of the dome of *in situ* XRD heating stage.

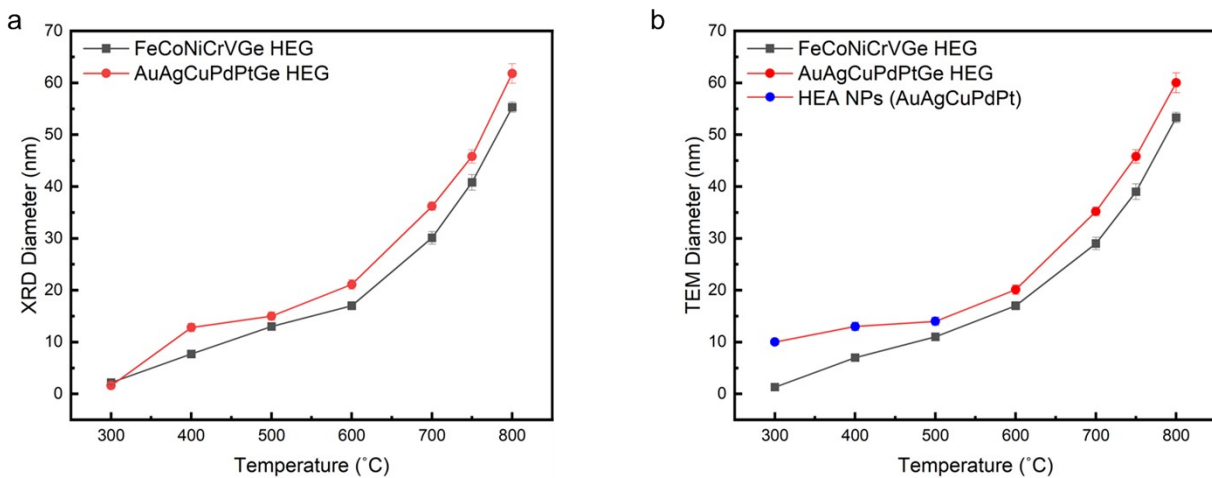


**Figure S18.** (a) Average size of HEGs derived from the XRD results and (b) average size of HEA NPs and HEG derived from the TEM results.

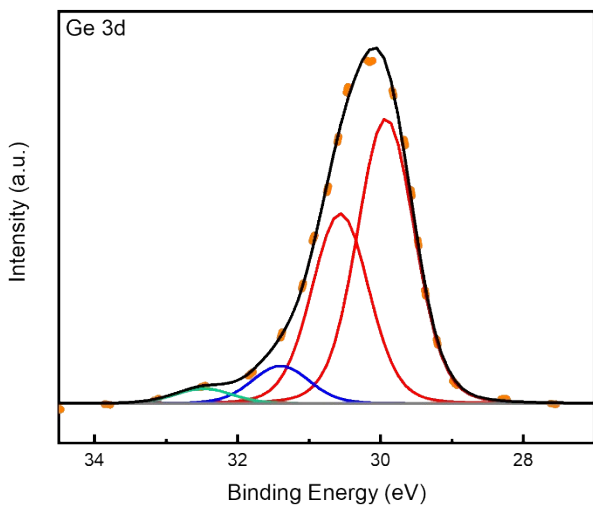


**Figure S19.** A representative high-resolution XP spectrum of Ge 3d region of metal salts&GeNSs precursor.

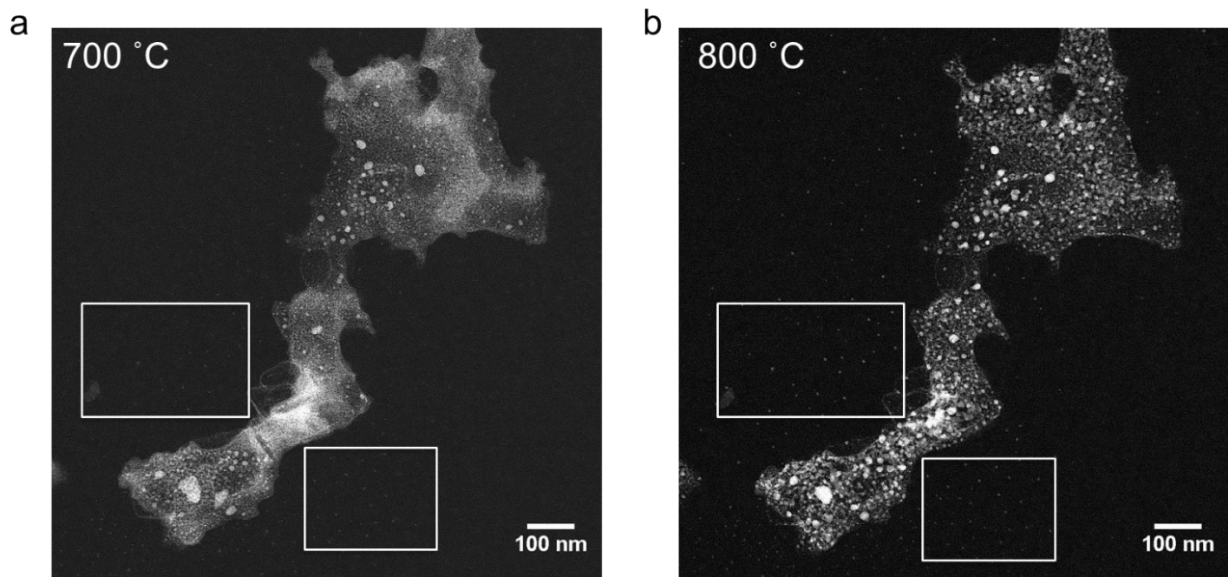


**Figure S20.** Enhanced HAADF-STEM images of FeCoNiCrVGe HEG at the same location during the *in situ* heating experiment at 700 °C and 800 °C. (Boxes highlight regions where small metal nanoparticles arising from the reduction of excess metal salts have formed on the *in situ* heating nanochip.)

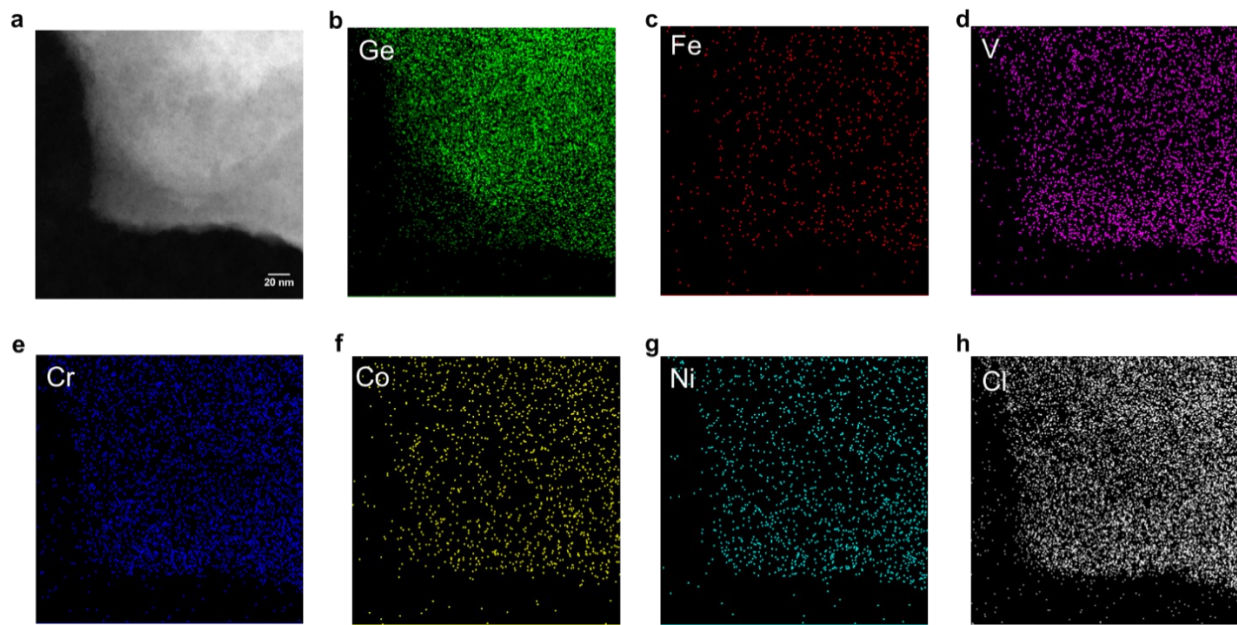


**Figure S21.** Representative HAADF-STEM images and EDX mapping of metal salts&GeNSs.

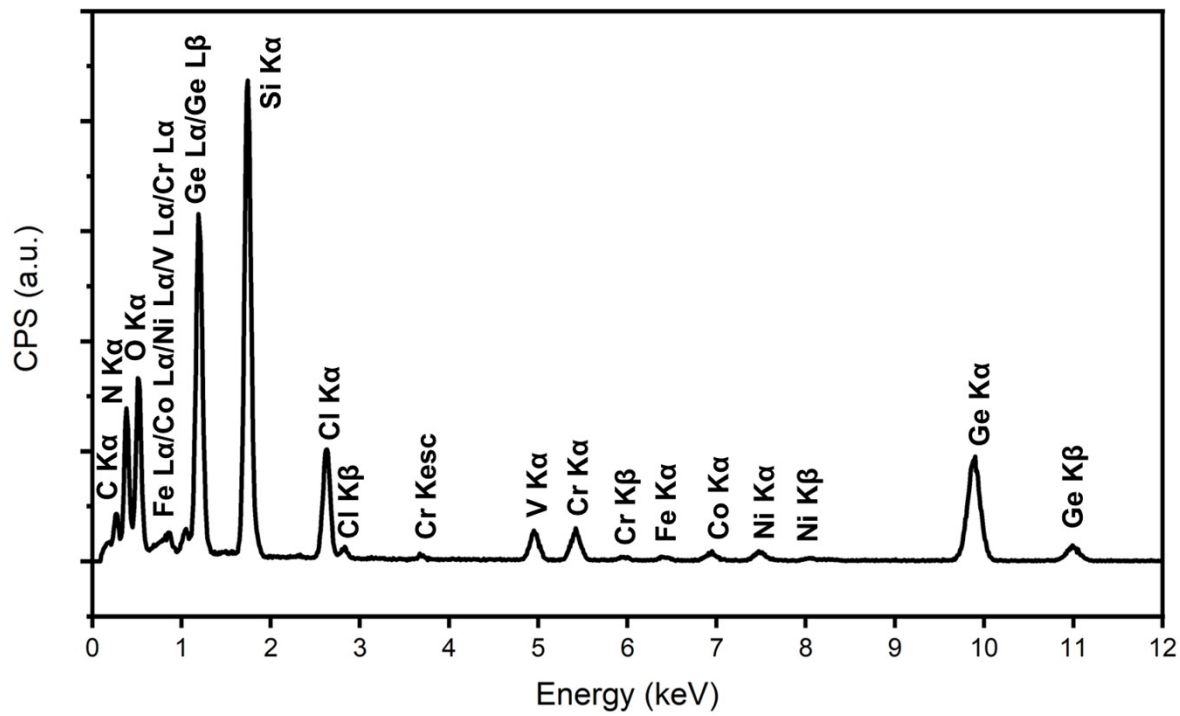


**Figure S22.** A Representative EDX spectrum for metal salts&GeNSs. Si and N signals result from the  $\text{Si}_3\text{N}_4$  chip.

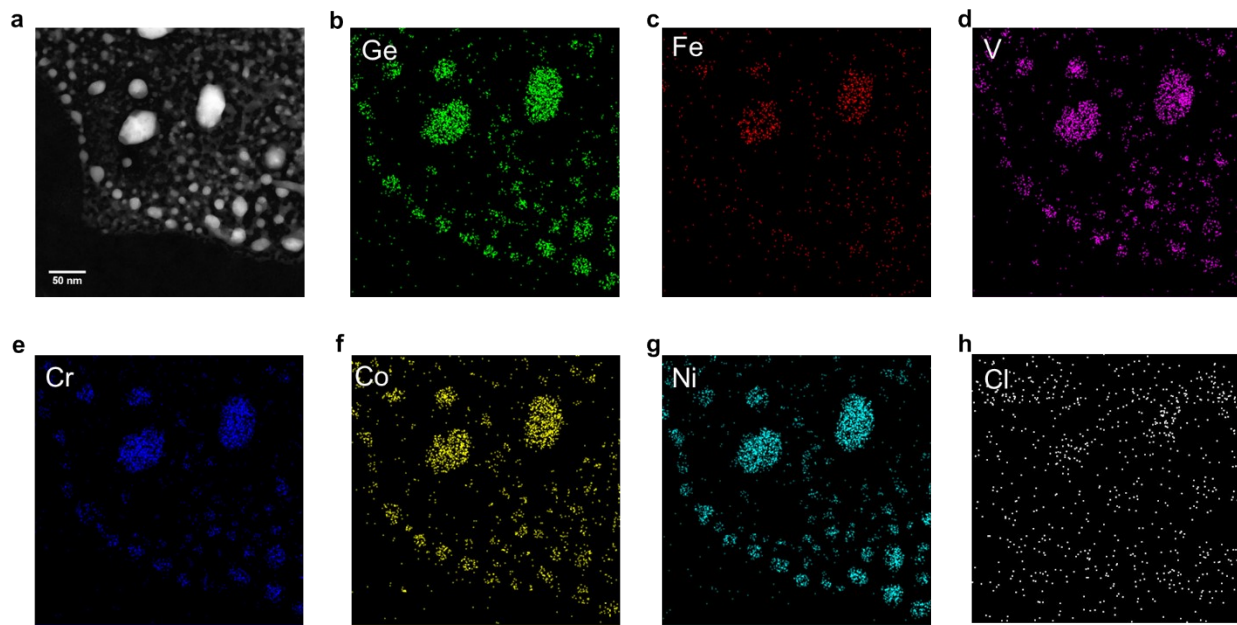


**Figure S23.** A representative HAADF-STEM images and EDX mapping of FeCoNiCrVGe HEG.

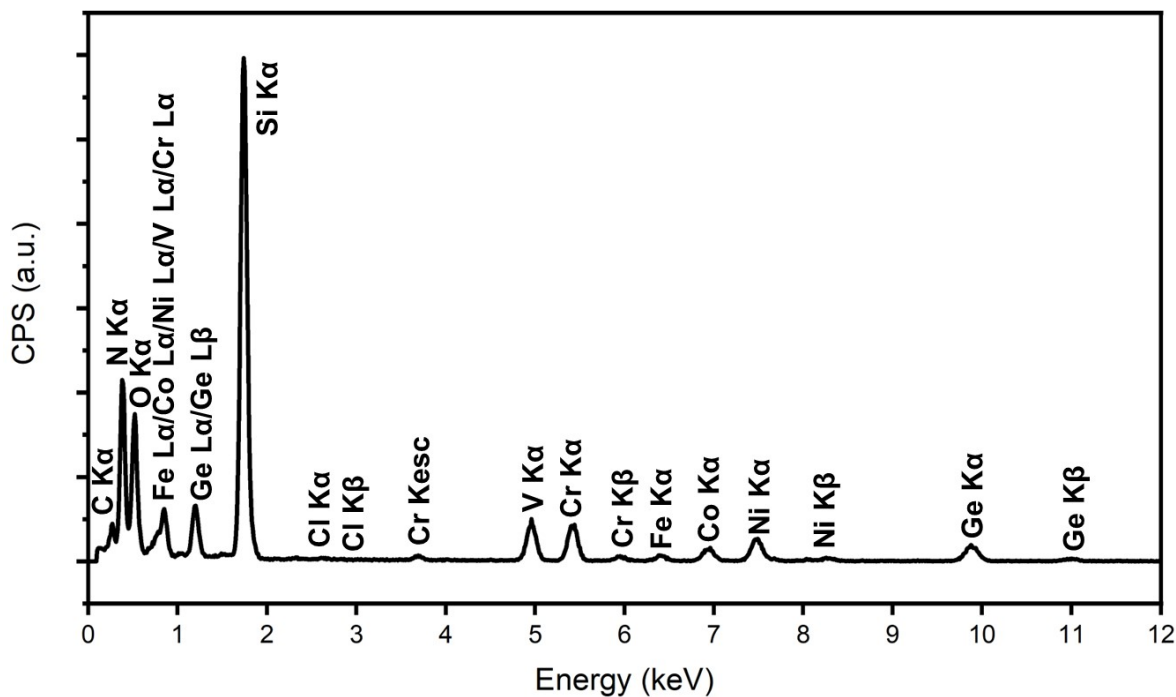


**Figure S24.** A Representative EDX spectrum for FeCoNiCrVGe HEG. Si and N signals result from the  $\text{Si}_3\text{N}_4$  chip.

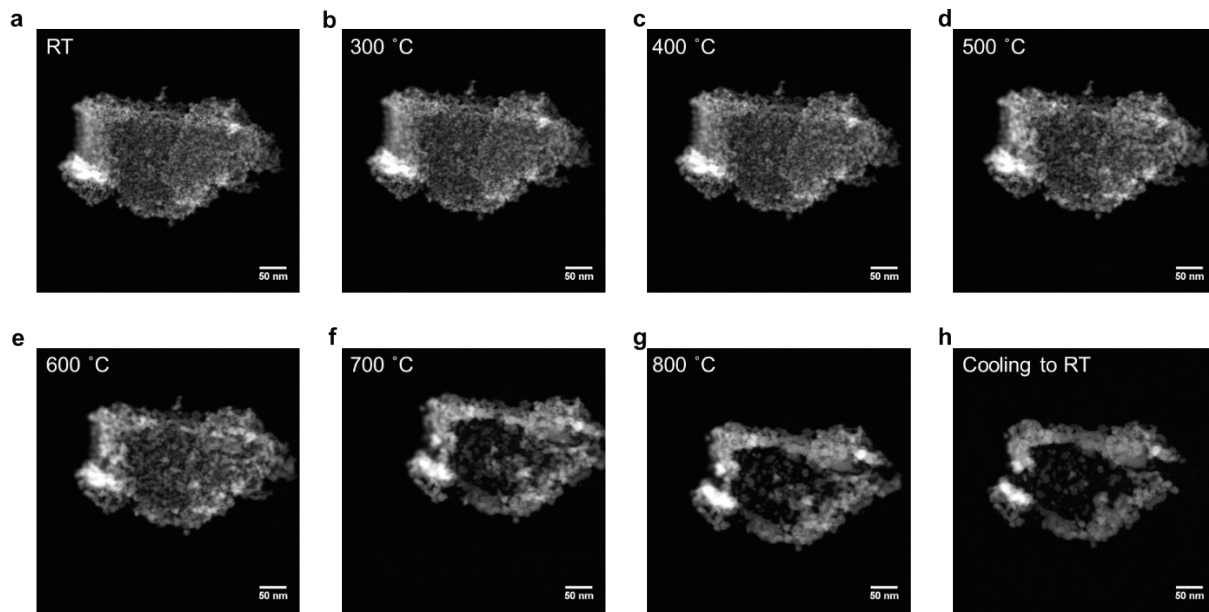


**Figure S25.** HAADF-STEM images of AuAgCuPdPtGe HEG at the same location during the *in situ* heating experiment from room temperature to 800 °C (a-g) and after cooling to room temperature (h). The sample shifted slightly due to thermal drift.

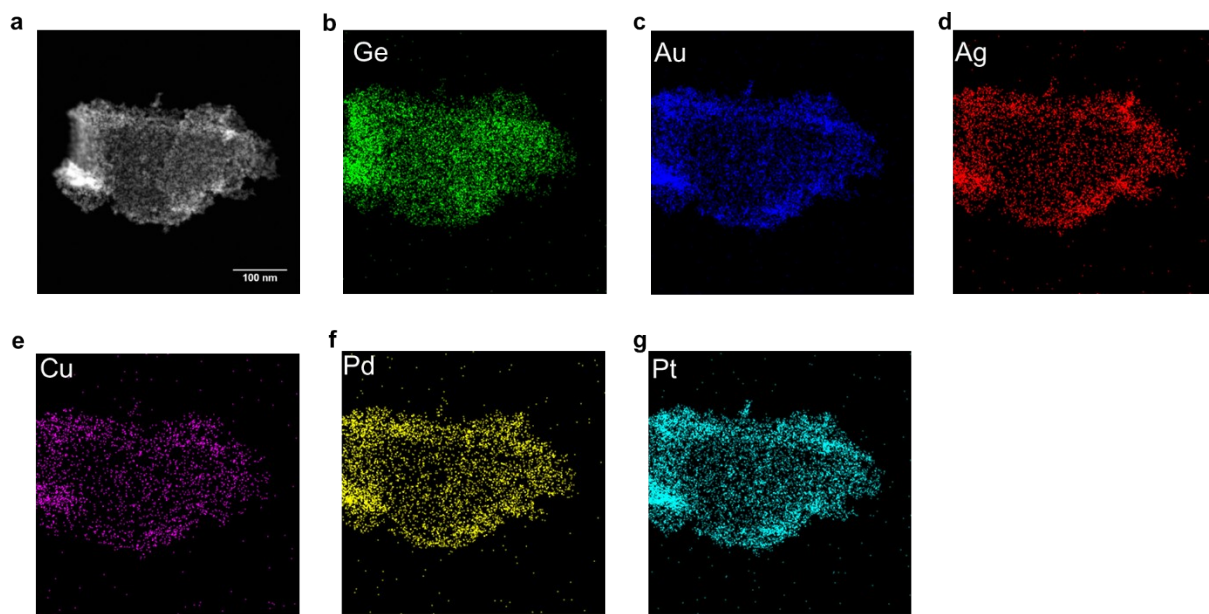


**Figure S26.** A representative HAADF-STEM images and EDX mapping of HEA NPs@GeNSs.

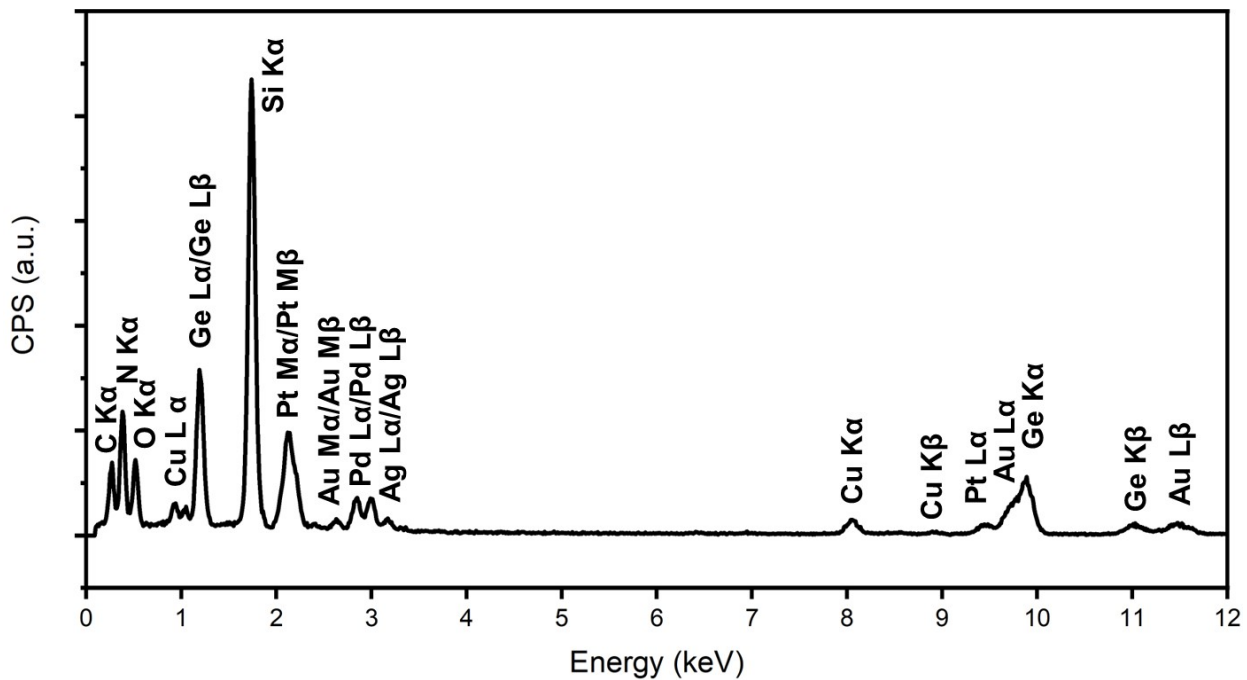


**Figure S27.** A representative EDX spectrum for HEA NPs@GeNSs. Si and N signals result from the  $\text{Si}_3\text{N}_4$  chip.

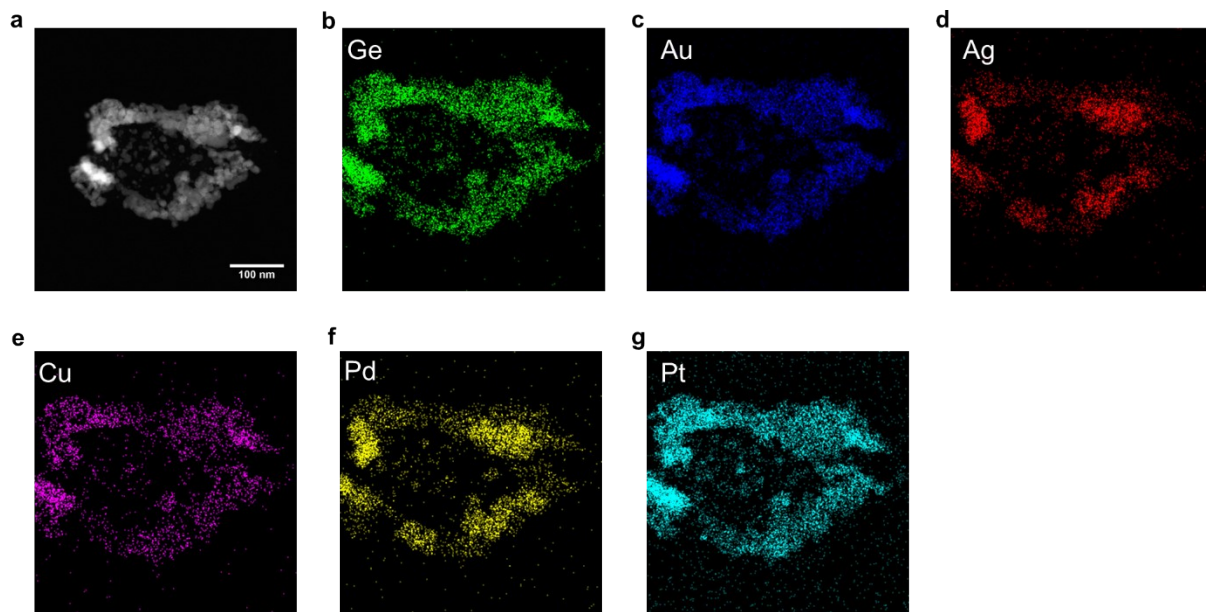


**Figure S28.** A representative HAADF-STEM images and EDX mapping of AuAgCuPdPtGe HEG.

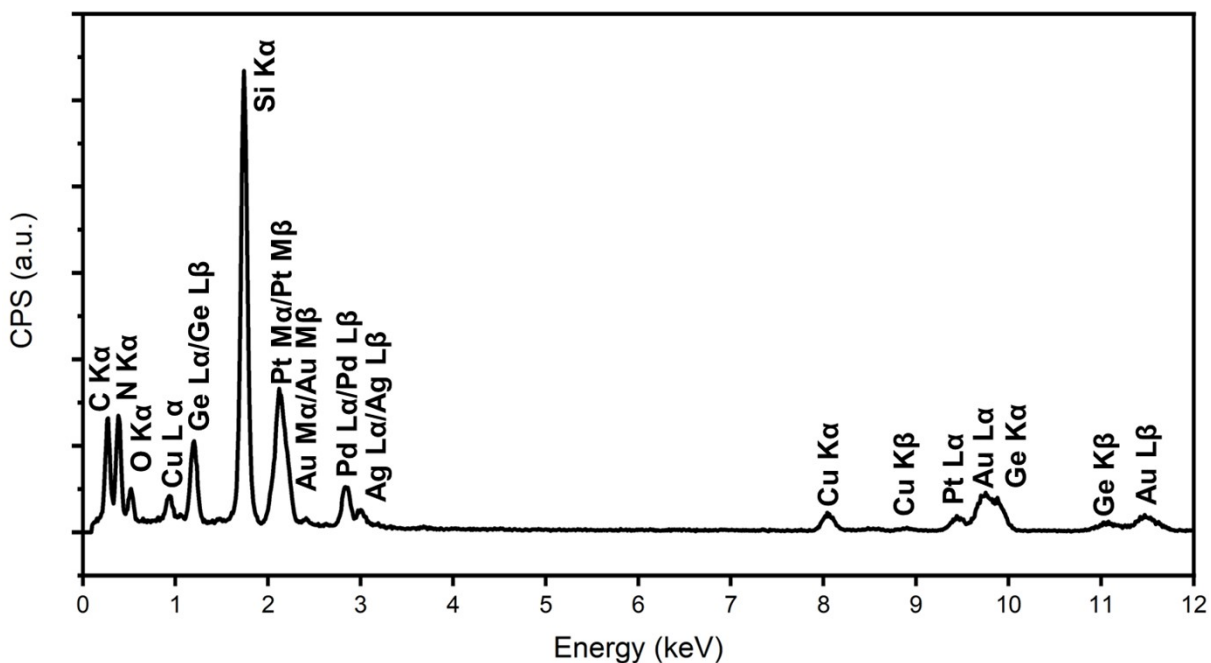


**Figure S29.** A representative EDX spectrum for AuAgCuPdPtGe HEG. Si and N signals result from the  $\text{Si}_3\text{N}_4$  chip.

## References

1. N. D. Cultrara, Y. Wang, M. Q. Arguilla, M. R. Scudder, S. Jiang, W. Windl, S. Bobev and J. E. Goldberger, *Chem. Mater.*, 2018, 30, 1335-1343.
2. NIST X-ray Photoelectron Spectroscopy Database, NIST Standard Reference Database Number 20, National Institute of Standards and Technology, Gaithersburg MD, 20899 (2000).
3. CRC Handbook of Chemistry and Physics (95th ed.), CRC Press (2014).